11-30-2012

Proteome Analyses of Strains Cyanothece ATCC 51142 and PCC 7822 of the Diazotrophic Cyanobacterium Cyanothece sp. Under Culture Conditions Resulting in Enhanced H2 Production.

Uma K. Aryal

Stephen J. Callister

Sujata Mishra

Xiaohui Zhang

Janani I. Shutthanandan

See next page for additional authors

Recommended Citation

Aryal, Uma K.; Callister, Stephen J.; Mishra, Sujata; Zhang, Xiaohui; Shutthanandan, Janani I.; Angel, Thomas E.; Shukla, Anil K.; Monroe, Matthew E.; Moore, Ronald J.; Koppenhaal, David W.; Smith, Richard D.; and Sherman, Louis A., "Proteome Analyses of Strains Cyanothece ATCC 51142 and PCC 7822 of the Diazotrophic Cyanobacterium Cyanothece sp. Under Culture Conditions Resulting in Enhanced H2 Production." (2012). *Department of Biological Sciences Faculty Publications.* Paper 36.
http://dx.doi.org/10.1128/AEM.02864-12

Authors
Uma K. Aryal, Stephen J. Callister, Sujata Mishra, Xiaohui Zhang, Janani I. Shutthanandan, Thomas E. Angel, Anil K. Shukla, Matthew E. Monroe, Ronald J. Moore, David W. Koppenhaal, Richard D. Smith, and Louis A. Sherman

Applied and Environmental Microbiology

Proteome Analyses of Strains ATCC 51142 and PCC 7822 of the Diazotrophic Cyanobacterium Cyanothece sp. under Culture Conditions Resulting in Enhanced H_2 Production

Uma K. Aryal, Stephen J. Callister, Sujata Mishra, Xiaohui Zhang, Janani I. Shutthanandan, Thomas E. Angel, Anil K. Shukla, Matthew E. Monroe, Ronald J. Moore, David W. Koppenaal, Richard D. Smith and Louis Sherman

Appl. Environ. Microbiol. **2013, 79(4):1070. DOI: 10.1128/AEM.02864-12.**
Published Ahead of Print 30 November 2012.

AEM
Journals.ASM.org

Proteome Analyses of Strains ATCC 51142 and PCC 7822 of the Diazotrophic Cyanobacterium *Cyanothece* sp. under Culture Conditions Resulting in Enhanced H_2 Production

Uma K. Aryal,[a]* Stephen J. Callister,[a] Sujata Mishra,[b] Xiaohui Zhang,[b] Janani I. Shutthanandan,[a] Thomas E. Angel,[a]* Anil K. Shukla,[a] Matthew E. Monroe,[a] Ronald J. Moore,[a] David W. Koppenaal,[a] Richard D. Smith,[a] Louis Sherman[b]

Pacific Northwest National Laboratory, Richland, Washington, USA[a]; Department of Biological Sciences, Purdue University, West Lafayette, Indiana, USA[b]

Cultures of the cyanobacterial genus *Cyanothece* have been shown to produce high levels of biohydrogen. These strains are diazotrophic and undergo pronounced diurnal cycles when grown under N_2-fixing conditions in light-dark cycles. We seek to better understand the way in which proteins respond to these diurnal changes, and we performed quantitative proteome analysis of *Cyanothece* sp. strains ATCC 51142 and PCC 7822 grown under 8 different nutritional conditions. Nitrogenase expression was limited to N_2-fixing conditions, and in the absence of glycerol, nitrogenase gene expression was linked to the dark period. However, glycerol induced expression of nitrogenase during part of the light period, together with cytochrome *c* oxidase (Cox), glycogen phosphorylase (Glp), and glycolytic and pentose phosphate pathway (PPP) enzymes. This indicated that nitrogenase expression in the light was facilitated via higher levels of respiration and glycogen breakdown. Key enzymes of the Calvin cycle were inhibited in *Cyanothece* ATCC 51142 in the presence of glycerol under H_2-producing conditions, suggesting a competition between these sources of carbon. However, in *Cyanothece* PCC 7822, the Calvin cycle still played a role in cofactor recycling during H_2 production. Our data comprise the first comprehensive profiling of proteome changes in *Cyanothece* PCC 7822 and allow an in-depth comparative analysis of major physiological and biochemical processes that influence H_2 production in both strains. Our results revealed many previously uncharacterized proteins that may play a role in nitrogenase activity and in other metabolic pathways and may provide suitable targets for genetic manipulation that would lead to improvement of large-scale H_2 production.

Biofuels have drawn intense interest, but also sharp debate, due to uncertainty about the cost and supply of fossil fuels and concerns about greenhouse gas emissions (1). During the energy crisis of the 1970s, hydrogen (H_2) was touted as the "fuel of the future," and a great deal of research was conducted in this area until early 1990s (2). In recent years, this area of research has again received renewed interest to determine the technical and economic feasibility of H_2 production relative to the use of fossil fuels (3–6).

H_2 production in algae and bacteria basically relies on either photosynthetic or fermentative processes (7). Since the initial demonstration of *in vivo* H_2 production in *Anabaena cylindrica*, a nitrogen-fixing cyanobacterium (blue-green alga) (7), several photosynthetic microbes have been studied for H_2 production (4, 8–10). Recently, members of the cyanobacterial genus *Cyanothece*, composed of unicellular, diazotrophic strains, have been intensively studied for biofuel research. These strains demonstrated pronounced diurnal rhythms when grown under N_2-fixing conditions in 12-h light-dark (LD) cycles or even in continuous light. *Cyanothece* strains perform photosynthesis in the light and store the fixed CO_2 in large glycogen granules. In turn, this glycogen is used as a substrate for respiration in the dark. This respiration not only produces ATP but also removes much intracellular O_2 that might inactivate the O_2-sensitive nitrogenase (11, 12). More recently, this powerful nitrogenase system has been shown to produce high levels of H_2 under diazotrophic conditions (13, 14). Furthermore, the completion of the genomic sequences of 7 *Cyanothece* species and the resulting comparative genomic studies (13) have paved the way for exploring features and functions of the major metabolic pathways and cellular functions to determine the overall utility of this H_2 production system.

Cyanothece sp. strain ATCC 51142 was the first member in the genus to be sequenced (15), and subsequent functional genomics studies have revealed many interesting features at both the transcriptional (16–20) and proteomic (21–23) levels. However, this strain has proven to be refractory to straightforward genetic analysis, and we thus sought to find another strain with better overall properties. Of the 7 *Cyanothece* strains that we had sequenced, only *Cyanothece* sp. strain PCC 7822 demonstrated the capacity for reasonable levels of homologous recombination relative to nonhomologous recombination so that we could develop a system capable of knockout mutations (24). *Cyanothece* 7822 (13, 25–27) is a strain with large cells (over 6 μm in length) and with different pigmentation, since cells contain phycoerythrin, which imparts a brownish color to the cultures (13). It can produce large quantities

Received 18 September 2012 **Accepted** 20 November 2012
Published ahead of print 30 November 2012
Address correspondence to Louis Sherman, lsherman@purdue.edu.
* Present address: Uma K. Aryal, Department of Biochemistry, Purdue University, West Lafayette, Indiana, USA; Thomas E. Angel, KineMed, Inc., Emeryville, California, USA.
Supplemental material for this article may be found at http://dx.doi.org/10.1128/AEM.02864-12.

doi:10.1128/AEM.02864-12

of organic acids, lipids, and polyhydroxyalkanoates (PHA) (25) and copious amounts of H_2 (24).

In this study, we analyzed protein changes due to alteration of three parameters: nitrogen-replete versus nitrogen-fixing conditions, ambient levels of CO_2 versus 50 mM glycerol, and each of these under continuous light (LL) versus 12-h light-dark (LD) conditions. We compared proteomes of the two strains under these conditions and demonstrated the value of proteomics for an understanding of biofuel production.

MATERIALS AND METHODS

Growth conditions. *Cyanothece* 7822 and *Cyanothece* 51142 were grown under 8 different conditions in 250-ml flasks on a shaker at 125 rpm at 30°C: in continuous light or 12 h light/12 h dark (50 μmol photons m^{-2} s^{-1}), in BG11 medium (for *Cyanothece* 7822) with or without $NaNO_3$ or in ASP2 medium (for *Cyanothece* 51142) with or without $NaNO_3$, and with or without glycerol. Cultures were grown to mid-log phase, and 200 ml cells was harvested after 3 days at 4 h into either the light period (L4) or the dark period (D4), frozen immediately in liquid nitrogen, stored at −80°C, and later used for protein extraction (see below). Some of the cells cultivated in BG11-NF or ASP-NF medium (without $NaNO_3$) were inoculated into a 6-liter bioreactor (Bioflo 3000; New Brunswick Scientific) and grown in 12 h light/12 h dark (100 μmol photons m^{-2} s^{-1} at 30°C) (20, 28). Measurements of nitrogenase and H_2 have been highly reproducible in this bioreactor over many years, and samples were taken from the bioreactor at various times through the diurnal cycle and used for the following measurements.

Assay for nitrogenase activity and H_2 production. Nitrogenase activity was measured by an acetylene reduction assay and expressed in terms of the ethylene produced (11). Acetylene reduction assays were carried out in 6.5-ml Becton Dickinson Vacutainer tubes. The tubes contained 2.0 ml of culture with 10% acetylene in the gas phase and were incubated at 30°C. After 1 h of incubation, 0.2 ml of 5 M NaOH was injected into each tube to stop the reaction. An aliquot of the gas phase (0.5 ml) was injected into a Hewlett-Packard series II gas chromatograph (GC) fitted with a Porapak N column and flame ionization detector. Gas flow rates of 30 ml of nitrogen, 30 ml of hydrogen, and 340 ml of air per min were used. The column and injector port temperatures were set at 100 and 150°C, respectively.

For H_2 production measurements, 10 ml of cells was incubated in 66-ml sealed glass vials at a light intensity of 50 μmol photons m^{-2} s^{-1} and 30°C for 24 h with shaking, either in air or sparged with argon in order to detect the highest rates of H_2 production. Gas samples (200 μl) were measured using a Hewlett-Packard 5890 series II GC with the same column and an oven temperature of 50°C and with a thermal conductivity detector at 100°C. Two technical replicates and three biological replicates were performed at each time point and analyzed for standard deviation. Total chlorophyll (Chl) *a* was extracted with methanol and quantified on a spectrophotometer (Lambda 40; Perkin-Elmer).

Protein extraction and proteolysis. Cells were pelleted by centrifugation at 8,000 × *g* for 5 min at 4°C. Cells were washed twice with 25 mM NH_4HCO_3 to remove any residual medium and resuspended in lysis buffer (2% SDS, 100 mM Tris-HCl [pH 8.0], 0.1% dithiothreitol [DTT], and 0.2% [vol/vol] protease inhibitor cocktail [Sigma-Aldrich, St. Louis, MO]). The reconstituted cells (200 μl) were transferred to a low-retention, 0.6-ml microcentrifuge tube, with 0.1 mm zirconia-silica beads added to the 0.6-ml mark, and placed in a Mini-Beadbeater (Bio Spec Products Inc.) for 3 min at 3,000 strokes/min. The cell lysate was collected by poking a hole in the base of the 0.6-ml microcentrifuge tube with a 26-gauge needle, nested inside an empty and decapped 1.5-ml microcentrifuge tube, and centrifuged for 5 min at 5,000 × *g* and 4°C. The beads were rinsed once with 200 μl of the same lysis buffer on top of the beads, placed in a new low-retention 1.5-ml microcentrifuge tube, and centrifuged for 5 min at 5,000 × *g* and 4°C. The cell lysates were pooled into one tube and centrifuged to remove whole cells or beads. Proteins were precipitated using 5 volumes of cold (−20°C) acetone, washed 3 times with 80% cold (−20°C) acetone, and resolubilized with 8 M urea. Protein concentrations were measured by using the bicinchoninic acid (BCA) assay (Pierce Chemical Co., Rockford, IL) and digested with trypsin as described elsewhere (23, 29, 30). Briefly, proteins were reduced by adding 5 mM freshly prepared DTT and incubating at 60°C for 30 min. Following incubation, all samples were diluted 5 times in 100 mM ammonium bicarbonate prior to tryptic digestion using sequencing-grade modified porcine trypsin (Promega, Madison, WI) at a 1:50 (wt/wt) trypsin-to-protein ratio for 5 h at 37°C. Peptides were desalted with C_{18} SPE columns (Supelco, St. Louis, MO) (31), concentrated to 100 μl in a Speed-Vac concentrator (GMI, Inc., Ramsey, MN), and monitored with a BCA assay.

Reverse-phase capillary LC-MS/MS analysis. Samples were analyzed using high-throughput hybrid liquid chromatography-tandem mass spectrometry (LC-MS/MS) as described previously (29, 32). A total of 6 μl (3 μg) of peptides from each replicate sample was analyzed using a custom-built automated four-column high-pressure capillary LC system coupled online to a linear ion trap (LTQ)-Orbitrap mass spectrometer (Thermo Fisher Scientific, San Jose, CA) via a nanoelectrospray ionization interface manufactured in-house (33, 34). The LC column was prepared by slurry packing 3-μm Jupiter C_{18} bonded particles (Phenomenex, Torrance, CA) into a 65-cm long, 75-μm-inner-diameter fused silica capillary (Polymicro Technologies, Phoenix, AZ). After 3 μg of peptides was loaded onto the column, the peptides were separated for a 100-min run using the following settings: 100% mobile phase solvent A (0.1% formic acid) for 20 min, followed by a linear gradient from 0 to 70% of solvent B (0.1% formic acid in 90% acetonitrile) over 80 min before reverting to 100% solvent A. From each full MS scan (*m/z* 400 to 2000), the 10 most abundant ions were selected for collision-induced dissociation (normalized collision energy setting of 35%) and MS/MS spectra generated per duty cycle. The dynamic exclusion window was set to 1 min, the heated capillary was maintained at 200°C, and the electrospray ionization (ESI) voltage was held at 2.2 kV.

Orthology determination. Orthologous *Cyanothece* 51142 and 7822 proteins were first predicted from the genome database using the InParanoid algorithm version 6 (http://InParanoid.sbc.su.se/) (35, 36) and were used to map the orthologous proteins identified in this study. The InParanoid program uses the pairwise similarity scores, calculated using NCBI BLAST, between two complete proteomes for constructing orthologous groups. Using this program, proteins are identified as orthologs if they have a reciprocal best BLAST hit score of at least 40, which has to be higher than a BLAST hit score to an outlier *Escherichia coli* genome, and the BLAST hit has a sequence alignment match of at least 50% in both proteins. Based on these criteria, ortholog groups were constructed by joining triangles of reciprocal best hits between two proteins.

Data analysis. LC-MS/MS raw data were converted into .dta files using Extract_MSn (version 4.0) in Bioworks Cluster 3.2 (Thermo Fisher Scientific, Cambridge, MA) and searched using the SEQUEST algorithm (v.27, Rev 12) against the completed genome sequence database for each strain from the Department of Energy Joint Genome Institute (http://img.jgi.doe.gov/cgi-bin/w/main.cgi), downloaded from the National Center for Biotechnology Information (NCBInr) on 21 February 2012. The SEQUEST output files (both forward and reverse hits) were imported to the Microsoft Office Access 2007 and filtered to achieve false-discovery rates (FDRs) of ≤0.4 at the peptide level and ≤2% at the protein level. The FDR was estimated using a decoy database search methodology (3) and MSGF spectral probabilities (37) of ≤1E−10. Proteins with two or more unique peptide identifications were retained for statistical analysis and hierarchical clustering.

The final output files were combined with treatment information, spectral count numbers, metabolic functions and, other relevant information in Microsoft Office Access 2007 and then loaded into Data Analysis Tool Extension (DAnTE) version 1.2 (38) for statistical analysis and clustering into heat maps. In DAnTE, the spectral count data were $\log_2$ transformed and normalized using the median absolute deviation adjustment

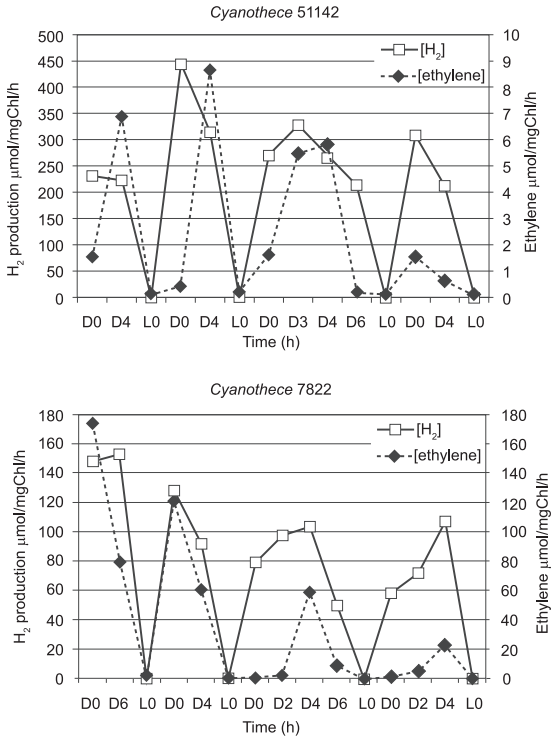

FIG 1 Hydrogen production and nitrogenase activity in *Cyanothece* 51142 (top) and *Cyanothece* 7822 (bottom). See Materials and Methods for details.

function and then subjected to analysis of variance (ANOVA). Proteins that were significantly different due to treatment were subjected to hierarchical clustering and visualized as heat maps.

RESULTS AND DISCUSSION

The periodicity of N_2 fixation and H_2 production is shown in Fig. 1. Both *Cyanothece* strains 51142 and 7822 were grown in the absence of combined nitrogen and under 12-h LD conditions, as detailed previously for *Cyanothece* 51142 (11). Nitrogenase activity usually peaked at 4 h into the dark period (D4) in *Cyanothece* 51142 and from D0, in the first cycle, to D4, in the remaining cycles, in *Cyanothece* 7822. The peak of H_2 production was also between D0 and D4 in both strains. The growth of both strains under N_2-fixing, LD conditions in the presence of 50 mM glycerol resulted in broader peaks (data not shown) that began in the light period, as shown previously (39). The results for cells grown in continuous light (LL) were similar to those reported previously (28) for *Cyanothece* 51142. Finally, the H_2 levels produced under nitrogen-replete conditions in both strains were much lower (~2 μmol H_2 produced/mg Chl/h), consistent with what has been shown previously (14).

Details of growth experiments and the total number of identified proteins are shown in Table 1. In *Cyanothece* 51142, the highest number of expressed proteins (786 proteins) was identified in sample A4 (without NO_3, without glycerol, and LD) and the lowest (534 proteins) in A5 (with NO_3, with glycerol, and LL), whereas the highest number of proteins (731) in *Cyanothece* 7822 was identified in A5 and the lowest (630) in A3 (without NO_3, with glycerol, and LL) (Table 1; see Tables S1 and S2 in the supplemental material). Thus, although the total observable proteomes were comparable between the two strains, their responses to the growth conditions were different. About a quarter of all the identified proteins could be classified as significantly ($P < 0.05$) different in amount among the 8 experiments (see Tables S3 and S4 in the supplemental material). Thus, proteins with higher spectral count measurement under a particular growth condition compared to the appropriate control (e.g., glycerol versus nonglycerol in LL or LD under N_2-fixing conditions) were defined as differentially upregulated proteins or vice versa. Using our criterion ($P \leq 0.05$), 173, 150, and 97 proteins were significantly different in *Cyanothece* 51142 in response to NO_3, glycerol, and light, whereas these values were 177, 93, and 91, respectively, for *Cyanothece* 7822. We also determined statistically significant proteins as a result of interaction between treatments (e.g., nitrate versus glycerol), as listed in Tables S3 and S4 in the supplemental material. The Venn diagrams in Fig. 2A and C summarize the distribution of statistically significant proteins among three treatments, with 43 proteins shared by all in *Cyanothece* 51142 and only 25 in *Cyanothece* 7822. Interestingly, 96 proteins that differ statistically in response to nitrate were unique to that treatment in *Cyanothece* 7822 (Fig. 2C). These statistically significant proteins were thought to play a key role in energy metabolism induced by growth conditions. Our analysis revealed that, under the experimental conditions used, the responses of *Cyanothece* 51142 and *Cyanothece* 7822 to glycerol were somewhat different, as evident from different number of statistically significant proteins detected in each treatment.

Functional categorization of the differentially expressed proteome based on the KEGG database showed that the categories with the largest number of expressed proteins in both strains were photosynthesis and respiration, translation, energy metabolism, amino acid biosynthesis, and cellular processes (Fig. 2B and D). Large numbers of statistically significant proteins could not be assigned, suggesting that it will be essential to identify more of these proteins currently annotated as unknown or hypothetical. Expression of several proteins belonging to photosynthesis, respiration, CO_2 fixation and assimilation, N_2 fixation, nitrogen assimilation, glycogen metabolism, glycolysis, oxidative pentose phosphate pathway (PPP), and fatty acid metabolism changed significantly in response to these treatments (see Tables S3 and S4 in the supplemental material). The most significant changes in protein expression were observed in both strains when they were grown with 50 mM glycerol under N_2-fixing conditions in LL.

Nitrogen fixation, H_2 production, and detoxification of O_2. The expression of nitrogenase proteins, including NifHDK, NifU,

TABLE 1 Total number of proteins identified under each set of growth conditions

Sample	Growth conditions[a]	Global proteome (no. of proteins) in strain:	
		ATCC 51142	PCC 7822
A1	−NO_3, +Gly, LL	618	658
A2	−NO_3, +Gly, LD	619	702
A3	−NO_3, −Gly, LL	778	630
A4	−NO_3, −Gly, LD	786	714
A5	+NO_3, +Gly, LL	534	731
A6	+NO_3, +Gly, LD	589	682
A7	+NO_3, −Gly, LL	685	707
A8	+NO_3, −Gly, LD	705	710

[a] −NO_3, without $NaNO_3$; +NO_3, with $NaNO_3$; −Gly, without glycerol; +Gly, with glycerol; LL, continuous light; LD, 12 h light/12 h dark.

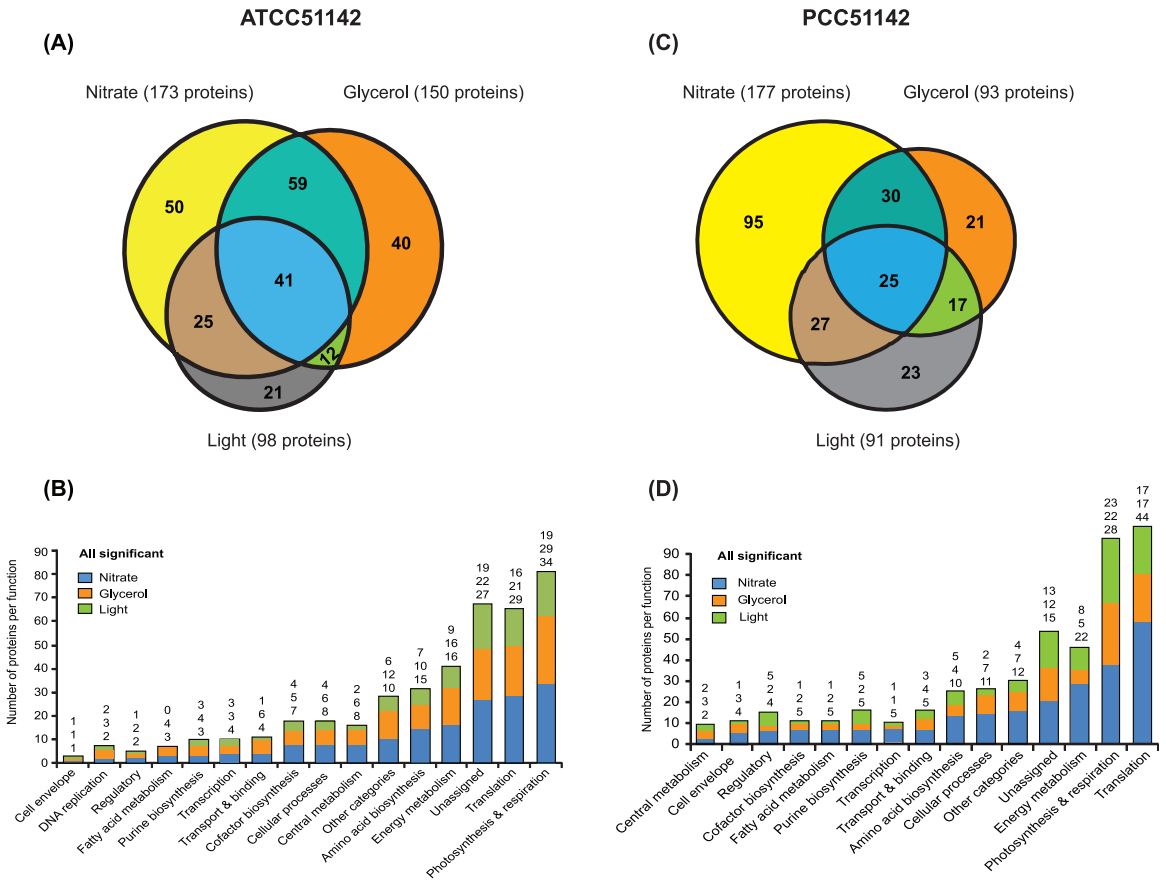

FIG 2 Comparison of *Cyanothece* 51142 and *Cyanothece* 7822 proteomic data. (A and C) Venn diagrams showing the overlap between significantly different proteins ($P \leq 0.05$) under nitrate, glycerol, and light for *Cyanothece* 51142 and *Cyanothece* 7822, respectively. Venn diagrams were plotted using Venn Diagram Plotter (http://omics.pnl.gov/software/VennDiagramPlotter.php). (B and D) Histograms showing functional classification of significantly different proteins based on KEGG pathway analysis (blue, nitrate; orange, glycerol; and green, light) for *Cyanothece* 51142 and *Cyanothece* 7822, respectively. The number of proteins in each functional group is shown on the top of each bar. The lists of these proteins for *Cyanothece* 51142 and 7822 are provided in Tables S3 and S4 in the supplemental material.

NifX, NifN, NifB, NifS, and NifW, was observed only under N_2-fixing conditions in both strains (Fig. 3), and in the absence of glycerol, their expression was strictly limited to the dark cycle, in accordance with previous results (21, 23). Interestingly, the glycerol-enhanced protein expression under N_2-fixing conditions was more pronounced when cells were grown under LL than under LD conditions. As expected, their expression was completely inhibited under nitrogen-sufficient conditions. In *Cyanothece* 51142, expression of DUF269 (gi|172035482, cce_0566) was observed exclusively under nitrogen-fixing conditions (see Table S1 in the supplemental material). The gene encoding DUF269 is located within the 35-gene *nif* gene cluster (15) and next to the *nifX* gene. This protein is only found in N_2-fixing bacteria and cyanobacteria and always next to *nifX*, clearly suggesting that it is an important protein for the construction of the nitrogenase enzyme.

Cyanothece 51142 and 7822 contain the *hupSL* genes for an uptake hydrogenase, and the genes are induced strongly in the dark under N_2-fixing conditions in *Cyanothece* 51142 (28) but to a lesser extent in *Cyanothece* 7822. Indeed, a low level of HupL was identified only in *Cyanothece* 51142 in this study (see Table S1 in the supplemental material). This is suggestive of weak uptake hydrogenase activity in *Cyanothece*, facilitating high H_2 production, as supported by studies of *hupL* mutants of *Anabaena* (10, 31, 40, 41). HupLS was not detected in *Cyanothece* 7822 under the conditions used in this study, another indication of their lower level of expression and lower activity. For both strains, the incubation in continuous light essentially ensured the absence of uptake hydrogenase activity. The bidirectional hydrogenase (encoded by *hox*) presumably plays a role during fermentation by utilizing excess reductant under anaerobic conditions (9, 42), and low levels of *hox* gene transcripts are known to be present under nitrogen-sufficient conditions (14). Expression of the 42-kDa soluble hydrogenase (cce_0379) was also independent of N_2-fixing growth conditions. This enzyme is involved in both production and consumption of H_2 (27, 43), including reductant disposal during fermentative metabolism in *Cyanothece* 7822 (25) and photo-H_2 production in *Chlorella focus* (44), but its role in aerobic H_2 production is not clear.

An interesting comparison between the two strains concerns the way that they balance and maintain redox and destroy oxidants. *Cyanothece* 51142 induces a peroxiredoxin to high levels in the dark to degrade reactive oxygen species (ROS) at the time of peak nitrogenase activity, whereas *Cyanothece* 7822 utilizes a different enzymatic process. Specifically, peroxiredoxin (cce_3126) was very strongly expressed in *Cyanothece* 51142, whereas the homologous protein in *Cyanothece* 7822 (Cyan7822_1871) was found at minimal levels. On

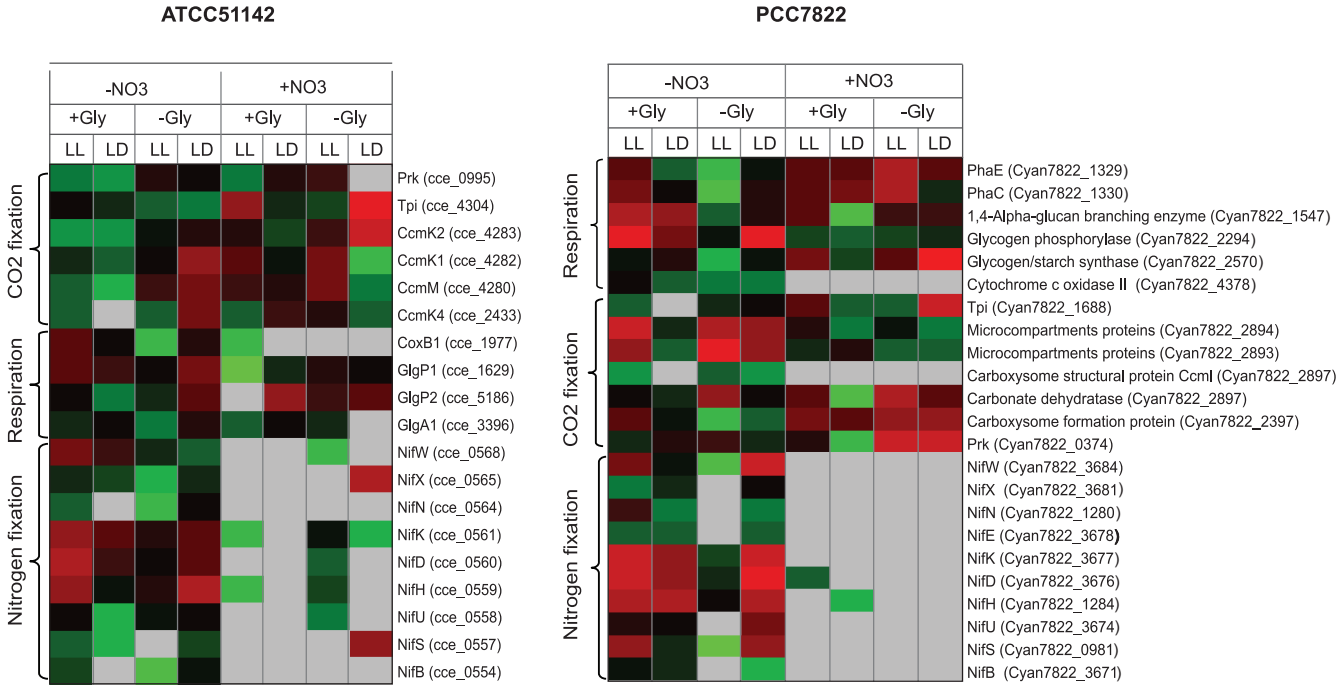

FIG 3 Examples of relative abundances of selected proteins under different growth conditions. Heat maps show the changes in the abundances of nitrogenase and other metabolic enzymes in *Cyanothece* 51142 (left) and *Cyanothece* 7822 (right). The protein symbols (or abbreviated protein names) with open reading frames (ORFs) are shown on the right.

the other hand, *Cyanothece* 7822 expressed much higher levels of thioredoxin peroxidase (Tpx; Cyan7822_3940 versus cce_2409). This suggests that the two strains have somewhat different strategies for removing O_2 radicals and ROS from the cytoplasm. As indicated in Fig. 1, nitrogenase activity decreased in *Cyanothece* 7822 from day 1 through day 4, whereas the extent of nitrogenase activity was both higher and more constant during the first 3 days in *Cyanothece* 51142. These results suggest that the high levels of the peroxiredoxin in *Cyanothece* 51142 may facilitate this response. Thus, one experiment to improve H_2 evolution in *Cyanothece* 7822 could be to replace the native promoter of the peroxiredoxin (Cyan7822_1871) with the peroxiredoxin promoter from *Cyanothece* 51142 and examine whether this leads to higher nitrogenase activity and concomitant H_2 evolution.

Glycerol metabolism. Expression of glycogen phosphorylase (GlgP1 [cce_1629] in *Cyanothece* 51142 and Cyan7822_2322 in *Cyanothece* 7822), the key enzyme for glycogen metabolism, was significantly upregulated in the presence of glycerol during diazotrophic growth (Fig. 3). However, GlgP2 (cce_5186) in *Cyanothece* 51142 was expressed under both nitrogen-fixing and nitrogen-sufficient conditions with no effect by glycerol. Similarly, cytochrome *c* oxidase (CoxB1; cce_1977 in *Cyanothece* 51142 and Cyan7822_4713 and Cyan7822_4378 in *Cyanothece* 7822), subunits of terminal oxidases in the respiratory transport chain, was also expressed exclusively under diazotrophic growth, and in the absence of glycerol, their abundance was higher in the dark cycle. However, similar to the case for nitrogenase, addition of glycerol increased expression of Cox in the light period, revealing that higher nitrogenase activity and H_2 production in continuous light growth are facilitated by higher respiration and glycogen metabolism. Expression of nitrogen-assimilatory proteins GlnA, ArgG, ArgD, and GlgF was also higher under nitrogen-fixing conditions, and their increased expression was positively correlated with N_2 fixation in both strains (see Tables S1 to S4 in the supplemental material).

Glycerol results in extensive reprogramming in *Cyanothece* 51142, particularly under H_2-producing conditions. This is seen as increased expression of genes needed for biomass growth, including genes for amino acid biosynthesis, purine, pyrimidine, and nucleotide synthesis, and the translational machinery (see Tables S1 to S4 in the supplemental material). Several ribosomal proteins are upregulated in response to glycerol. As growth increases, biosynthesis of amino acids is required, and as a consequence, the protein amount of a large fraction of such enzymes is also increased under glycerol. *Cyanothece* 51142 used the citramalate-dependent pathway to synthesize isoleucine when grown in glycerol (45), and we observed higher abundances of key proteins involved in this pathway when grown photoheterotrophically in glycerol. On the contrary, glycerol generated few metabolic changes in *Cyanothece* 7822. Both strains grow well mixotrophically, but with different metabolic consequences.

CO_2 fixation and assimilation. Expression of the Rubisco proteins (RbcLS) as well as other key CO_2 fixation proteins (CcmK1, CcmK2, CcmL, CcmM, and Prk) decreased in the presence of glycerol under both nitrate-depleted and -sufficient conditions in *Cyanothece* 51142 (Fig. 3, left panel; see Tables S1 and S3 in the supplemental material). This indicated that *Cyanothece* 51142 preferentially utilized additional carbon sources over photosynthetically fixed carbon for cellular metabolism. In agreement with this, *Cyanothece* 51142 cells have been shown previously to shift their metabolic strategy from mixotrophic or autotrophic growth to photoheterotrophic growth in the presence of glycerol (24, 46). In *Cyanothece* 51142, expression of other key enzymes of the CO_2 fixation pathway, IcfA1 (cce_2257), CmpA (cce_0305),

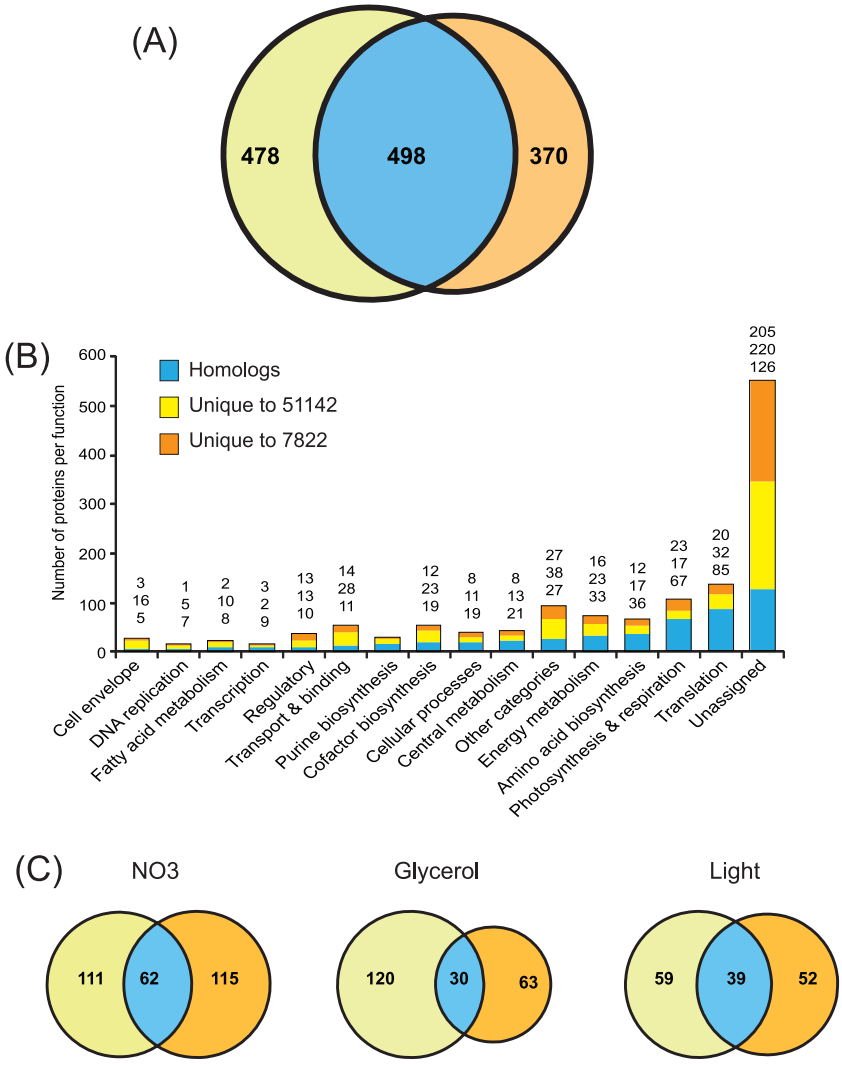

FIG 4 Comparison of the homologous relationship of expressed proteomes between *Cyanothece* 51142 and *Cyanothece* 7822. (A) Venn diagram showing proteins homologous between *Cyanothece* 51142 (yellow plus blue) and *Cyanothece* 7822 (orange plus blue). A list of these homologous proteins is shown in Table S5 in the supplemental material. (B) Histogram showing functional classification of the homologous and nonhomologous proteins. The number of proteins in each functional category is shown at the top of each bar. (C) Venn diagram showing the comparison of significantly different proteins ($P \leq 0.05$) for homologous and nonhomologous proteins. Homologous proteins were identified by comparing the current proteome data with the previously published, predicted homologous proteins based on genome sequence comparison (13).

SbtA (cce_2939), GlcE (cce_3707), and the ParA family chromosome-partitioning protein (cce_2448) also decreased in the presence of glycerol (Fig. 3, left panel; see Table S1 in the supplemental material). CmpA participates in the cotransport of bicarbonate, Ca^{2+}, and Na^{+} (47), whereas GlcE is a key enzyme to convert 2-phosphoglycolate to phosphatidylglycerol (PG) and O_2 (48). Recently, in *Synechococcus elongatus* PCC 7942, a *parA*-like gene (*Synpcc7942_1833*) was shown to control carboxysome organization (49). The fact that most of the carboxysome proteins were inhibited in the presence of glycerol in *Cyanothece* 51142 suggested that cells can directly utilize glycerol as a carbon source under N_2-fixing conditions (39).

Cyanothece 51142 can also fix CO_2 via anaplerotic pathways (i.e., C_4 carbon fixation) (50), but enzymes such as phosphoenolpyruvate (PEP) carboxylase (Ppc), PEP carboxykinase, or malic oxidoreductase (cce_3242) did not change in the presence of glycerol (see Table S1 in the supplemental material). This suggested that CO_2 was not utilized for the synthesis of C_4 metabolites in the tricarboxylic acid (TCA) cycle via anaplerotic pathways, such as oxaloacetate and succinate, which are precursors for chlorophyll biosynthesis (45, 46). Interestingly, the response of *Cyanothece* 7822 to glycerol for CO_2 fixation was quite different, as key Calvin cycle enzymes, including RbcLS and the Ccm proteins (microcompartment proteins), were generally expressed constitutively in the presence of glycerol. Overall, these proteins showed very little change among all eight growth conditions, suggesting that the mechanisms of carbohydrate metabolism are different in the two strains. In addition, the expression of Ppc was observed only under N_2-fixing conditions and glycerol had no influence in its expression, similar to the situation in *Cyanothece* 51142.

Energy metabolism. As expected (21–23), key enzymes of glycolysis, TCA cycle, and PPP showed higher level of expression under

N_2-fixing conditions than under nitrogen-sufficient conditions (see Tables S1 to S4 in the supplemental material), and their expression was further induced by the addition of glycerol under N_2-fixing conditions. Specifically, enzymes involved in the oxidative PPPs, including Zwf, Gnd, TktA, OpcA, TalA, and Pgl, were expressed with higher abundances under N_2-fixing conditions, and the addition of glycerol further induced expression of most of these enzymes, indicating significant activation of the PPP under H_2-producing culture conditions. Different chaperones, detoxifying proteins, cofactor biosyntheses, and protein degradations were also differentially expressed (see Tables S1 to S4 in the supplemental material), suggesting that they undergo targeted degradation. Phosphate ABC transporters exhibited increased expression under N_2-fixing conditions, and glycerol further increased their expression (see Tables S1 and S2 in the supplemental material).

Proteome comparison between the two strains. Comparison of homologous proteins between these two strains showed that >50% of the expressed proteome were homologous to each other (Fig. 4A). These shared homologous proteins encompass a range of metabolic and biochemical functions, including photosynthesis, respiration, CO_2 fixation, N_2 fixation, H_2 production, and energy metabolism (Fig. 4B). Functional classification of unique proteins (Fig. 4B) revealed that the majority belonged to hypothetical (unassigned), other categories, regulatory function, cofactor biosynthesis, or proteins involved in transport and binding, suggesting that these two strains differ mainly in secondary processes. The genome of *Cyanothece* 51142 includes an operon with one gene of PsaA and PsaB, whereas 7822 contains PsaA (Cyan7822_4990) and two very similar PsaB genes (Cyan7822_4988 and Cyan7822_4989). Importantly, both PsaB proteins were detected in *Cyanothece* 7822. Similarly, *Cyanothece* 7822 showed expression of hemerythrin HHE cation binding domain proteins (Cyan7822_2971 and Cyan7822_5288). In addition to homologous phycobiliproteins, some phycobiliproteins and phycobilisome (PBS) linker polypeptides detected in *Cyanothece* 7822 had no homologous proteins in *Cyanothece* 51142 (see Table S5 in the supplemental material), likely suggesting their link with phycoerythrin assembly and stability. Similarly, *Cyanothece* 7822 is capable of producing and storing large quantities of PHA, whereas *Cyanothece* 51142 lacks the necessary enzymes. We were able to detect the expression of the key enzymes PhaCE (Cyan7822_1329 and Cyan7822_1329) under all conditions. Protein expression was lower in the absence of nitrate and lowest in the absence of both nitrate and glycerol. Interestingly, the protein levels were highest in the presence of nitrate but in the absence of glycerol (see Table S4 in the supplemental material).

Conclusions. This study has illuminated the changes in protein composition of two species of cyanobacteria under 8 growth conditions. We could thus analyze the changing proteome relative to changes in combined nitrogen, to the addition of glycerol, and to different light cycles. Of particular interest, these proteome data demonstrated how glycerol modulated the synthesis of enzymes involved in multiple metabolic and biochemical processes. Higher abundances of CoxB1 and GlgP1 in *Cyanothece* 51142 and *Cyanothece* 7822 in the presence of glycerol under H_2-producing conditions suggested that cells maintained suboxic condition for nitrogenase activities by higher levels of respiration and glycogen metabolism. We also detected differences in the way the two strains detoxify ROS from the cytoplasm during N_2 fixation.

Changes in protein abundances reflect changes in cellular strategy. Based on information about protein abundance changes, we provide a simple overview of cellular metabolism of *Cyanothece* 51142 in the presence of glycerol under N_2-fixing condition and continuous light (Fig. 5). The activation (black arrows with red blocks) or inhibition (gray arrows) of the pathway was based on the increase or decrease of key enzymes in the pathway. The main carbon metabolic route was similar for both strains, as homologous proteins in this route were correlated. However, differences in metabolism were also mirrored in protein abundances, particularly for key enzymes of CO_2 fixation.

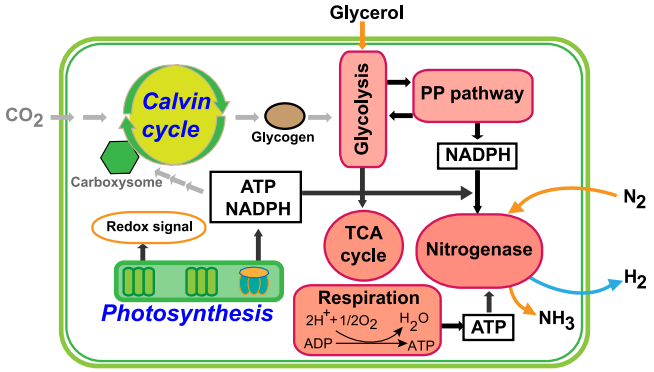

FIG 5 Overview of the cellular metabolism and redox balancing in *Cyanothece* 51142 in the presence of glycerol under N_2-fixing conditions. The biochemical pathways were predicted based on the current proteomic data. Arrows show the direction of the reaction. Gray arrows indicate the decrease and black arrows with red blocks indicate the increase in metabolic activity. The biochemical pathway of *Cyanothece* 7822 for the main route of carbon metabolism (black arrows and red blocks) was similar, but that for CO_2 fixation (gray arrows) was different. While key proteins involved in CO_2 fixation decreased in *Cyanothece* 51142, corresponding homologous proteins in *Cyanothece* 7822 increased in the presence of glycerol.

ACKNOWLEDGMENTS

This work was supported by a grant from the DOE Genomics:GTL program, and a portion of the research was performed using EMSL, a national scientific user facility sponsored by the Department of Energy's Office of Biological and Environmental Research and located at Pacific Northwest National Laboratory.

REFERENCES

1. **Alper H, Stephanopoulos G.** 2009. Engineering for biofuels: exploiting innate microbial capacity or importing biosynthetic potential? Nat. Rev. Microbiol. **7**:715–723.
2. **Benemann J.** 1996. Hydrogen biotechnology: progress and prospects. Nat. Biotechnol. **14**:1101–1103.
3. **Ghirardi ML, Mohanty P.** 2010. Oxygenic hydrogen photoproduction—current status of the technology. Curr. Sci. India **98**:499–507.
4. **Ghirardi ML, Zhang JP, Lee JW, Flynn T, Seibert M, Greenbaum E, Melis A.** 2000. Microalgae: a green source of renewable H-2. Trends Biotechnol. **18**:506–511.
5. **Hallenbeck PC, Ghosh D.** 2009. Advances in fermentative biohydrogen production: the way forward? Trends Biotechnol. **27**:287–297.
6. **Kruse O, Rupprecht J, Mussgnug JH, Dismukes GC, Hankamer B.** 2005. Photosynthesis: a blueprint for solar energy capture and biohydrogen production technologies. Photochem. Photobiol. Sci. **4**:957–970.
7. **Benemann JR, Weare NM.** 1974. Hydrogen evolution by nitrogen-fixing Anabaena cylindrica cultures. Science **184**:174–175.
8. **Mitsui A, Kumazawa S, Takahashi A, Ikemoto H, Cao S, Arai T.** 1986. Strategy by which nitrogen-fixing unicellular cyanobacteria grow photoautotrophically. Nature **323**:720–722.
9. **Tamagnini P, Axelsson R, Lindberg P, Oxelfelt F, Wunschiers R, Lindblad P.** 2002. Hydrogenases and hydrogen metabolism of cyanobacteria. Microbiol. Mol. Biol. Rev. **66**:1.

10. **Tamagnini P, Leitao E, Oliveira P, Ferreira D, Pinto F, Harris DJ, Heidorn T, Lindblad P.** 2007. Cyanobacterial hydrogenases: diversity, regulation and applications. FEMS Microbiol. Rev. **31**:692–720.
11. **Schneegurt MA, Sherman DM, Nayar S, Sherman LA.** 1994. Oscillating behavior of carbohydrate granule formation and dinitrogen fixation in the cyanobacterium Cyanothece sp. strain ATCC 51142. J. Bacteriol. **176**: 1586–1597.
12. **Sherman LA, Meunier P, Colon-Lopez MS.** 1998. Diurnal rhythms in metabolism: a day in the life of a unicellular, diazotrophic cyanobacterium. Photosynth. Res. **58**:25–42.
13. **Bandyopadhyay A, Elvitigala T, Welsh E, Stockel J, Liberton M, Min H, Sherman LA, Pakrasi HB.** 2011. Novel metabolic attributes of the genus *Cyanothece*, comprising a group of unicellular nitrogen-fixing cyanobacteria. mBio **2**:e00214-11. doi:10.1128/mBio.00214-11.
14. **Min H, Sherman LA.** 2010. Hydrogen production by the unicellular, diazotrophic cyanobacterium Cyanothece sp. strain ATCC 51142 under conditions of continuous light. Appl. Environ. Microbiol. **76**:4293–4301.
15. **Welsh EA, Liberton M, Stockel J, Loh T, Elvitigala T, Wang C, Wollam A, Fulton RS, Clifton SW, Jacobs JM, Aurora R, Ghosh BK, Sherman LA, Smith RD, Wilson RK, Pakrasi HB.** 2008. The genome of Cyanothece 51142, a unicellular diazotrophic cyanobacterium important in the marine nitrogen cycle. Proc. Natl. Acad. Sci. U. S. A. **105**:15094–15099.
16. **Elvitigala T, Stockel J, Ghosh BK, Pakrasi HB.** 2009. Effect of continuous light on diurnal rhythms in Cyanothece sp. ATCC 51142. BMC Genomics **10**:226.
17. **Singh AK, Elvitigala T, Bhattacharyya-Pakrasi M, Aurora R, Ghosh B, Pakrasi HB.** 2008. Integration of carbon and nitrogen metabolism with energy production is crucial to light acclimation in the cyanobacterium Synechocystis. Plant Physiol. **148**:467–478.
18. **Singh AK, Elvitigala T, Cameron JC, Ghosh BK, Bhattacharyya-Pakrasi M, Pakrasi HB.** 2010. Integrative analysis of large scale expression profiles reveals core transcriptional response and coordination between multiple cellular processes in a cyanobacterium. BMC Syst. Biol. **4**:105.
19. **Stockel J, Welsh EA, Liberton M, Kunnvakkam R, Aurora R, Pakrasi HB.** 2008. Global transcriptomic analysis of Cyanothece 51142 reveals robust diurnal oscillation of central metabolic processes. Proc. Natl. Acad. Sci. U. S. A. **105**:6156–6161.
20. **Toepel J, Welsh E, Summerfield TC, Pakrasi HB, Sherman LA.** 2008. Differential transcriptional analysis of the cyanobacterium Cyanothece sp. strain ATCC 51142 during light-dark and continuous-light growth. J. Bacteriol. **190**:3904–3913.
21. **Aryal UK, Stockel J, Krovvidi RK, Gritsenko MA, Monroe ME, Moore RJ, Koppenaal DW, Smith RD, Pakrasi HB, Jacobs JM.** 2011. Dynamic proteomic profiling of a unicellular cyanobacterium Cyanothece ATCC51142 across light-dark diurnal cycles. BMC Syst. Biol. **5**:194.
22. **Aryal UK, Stockel J, Welsh EA, Gritsenko MA, Nicora CD, Koppenaal DW, Smith RD, Pakrasi HB, Jacobs JM.** 2012. Dynamic proteome analysis of Cyanothece sp. ATCC 51142 under constant light. J. Proteome Res. **11**:609–619.
23. **Stockel J, Jacobs JM, Elvitigala TR, Liberton M, Welsh EA, Polpitiya AD, Gritsenko MA, Nicora CD, Koppenaal DW, Smith RD, Pakrasi HB.** 2011. Diurnal rhythms result in significant changes in the cellular protein complement in the cyanobacterium Cyanothece 51142. PLoS One **6**:e16680. doi:10.1371/journal.pone.0016680.
24. **Min HT, Sherman LA.** 2010. Genetic transformation and mutagenesis via single-stranded DNA in the unicellular, diazotrophic cyanobacteria of the genus Cyanothece. Appl. Environ. Microbiol. **76**:7641–7645.
25. **Vanderoost J, Bulthuis BA, Feitz S, Krab K, Kraayenhof R.** 1989. Fermentation metabolism of the unicellular cyanobacterium Cyanothece PCC 7822. Arch. Microbiol. **152**:415–419.
26. **Vanderoost J, Cox RP.** 1989. Hydrogenase activity in nitrate-grown cells of the unicellular cyanobacterium Cyanothece PCC 7822. Arch. Microbiol. **151**:40–43.
27. **Vanderoost J, Kanneworff WA, Krab K, Kraayenhof R.** 1987. Hydrogen metabolism of 3 unicellular nitrogen-fixing cyanobacteria. FEMS Microbiol. Lett. **48**:41–45.
28. **Toepel J, McDermott JE, Summerfield TC, Sherman LA.** 2009. Transcriptional analysis of the unicellular, diazotrophic cyanobacterium Cyanothece sp ATCC 51142 grown under short day/night cycles. J. Phycol. **45**:610–620.
29. **Jacobs JM, Mottaz HM, Yu LR, Anderson DJ, Moore RJ, Chen WNU, Auberry KJ, Strittmatter EF, Monroe ME, Thrall BD, Camp DG, Smith RD.** 2004. Multidimensional proteome analysis of human mammary epithelial cells. J. Proteome Res. **3**:68–75.
30. **Wegener KM, Singh AK, Jacobs JM, Elvitigala T, Welsh EA, Keren N, Gritsenko MA, Ghosh BK, Camp DG, II, Smith RD, Pakrasi HB.** 2010. Global proteomics reveal an atypical strategy for carbon/nitrogen assimilation by a cyanobacterium under diverse environmental perturbations. Mol. Cell. Proteomics **9**:2678–2689.
31. **Dutta D, De D, Chaudhuri S, Bhattacharya SK.** 2005. Hydrogen production by cyanobacteria. Microb. Cell Factories **4**:36.
32. **Jacobs JM, Diamond DL, Chan EY, Gritsenko MA, Qian WJ, Stastna M, Baas T, Camp DG, Carithers RL, Smith RD, Katze MG.** 2005. Proteome analysis of liver cells expressing a full-length hepatitis C virus (HCV) replicon and biopsy specimens of posttransplantation liver from HCV-infected patients. J. Virol. **79**:7558–7569.
33. **Shen Y, Tolic N, Masselon C, Pasa-Tolic L, Camp DG, Hixson KK, Zhao R, Anderson GA, Smith RD.** 2004. Ultrasensitive proteomics using high-efficiency on-line micro-SPE-NanoLC-NanoESI MS and MS/MS. Anal. Chem. **76**:144–154.
34. **Shen YF, Jacobs JM, Camp DG, Fang RH, Moore RJ, Smith RD, Xiao WZ, Davis RW, Tompkins RG.** 2004. Ultra-high-efficiency strong cation exchange LC/RPLC/MS/MS for high dynamic range characterization of the human plasma proteome. Anal. Chem. **76**:1134–1144.
35. **Remm M, Storm CE, Sonnhammer EL.** 2001. Automatic clustering of orthologs and in-paralogs from pairwise species comparisons. J. Mol. Biol. **314**:1041–1052.
36. **Sonnhammer ELL, Koonin EV.** 2002. Orthology, paralogy and proposed classification for paralog subtypes. Trends Genet. **18**:619–620.
37. **Kim S, Gupta N, Pevzner PA.** 2008. Spectral probabilities and generating functions of tandem mass spectra: a strike against decoy databases. J. Proteome Res. **7**:3354–3363.
38. **Polpitiya AD, Qian WJ, Jaitly N, Petyuk VA, Adkins JN, Camp DG, Anderson GA, Smith RD.** 2008. DAnTE: a statistical tool for quantitative analysis of -omics data. Bioinformatics **24**:1556–1558.
39. **Bandyopadhyay A, Stockel J, Min H, Sherman LA, Pakrasi HB.** 2010. High rates of photobiological H_2 production by a cyanobacterium under aerobic conditions. Nat. Commun. **1**:139.
40. **Asada Y, Kawamura S.** 1986. Aerobic hydrogen accumulation by a nitrogen-fixing cyanobacterium, Anabaena sp. Appl. Environ. Microbiol. **51**: 1063–1066.
41. **Masukawa H, Mochimaru M, Sakurai H.** 2002. Disruption of the uptake hydrogenase gene, but not of the bidirectional hydrogenase gene, leads to enhanced photobiological hydrogen production by the nitrogen-fixing cyanobacterium Anabaena sp PCC 7120. Appl. Microbiol. Biotechnol. **58**:618–624.
42. **Bryant DA, Frigaard NU.** 2006. Prokaryotic photosynthesis and phototrophy illuminated. Trends Microbiol. **14**:488–496.
43. **Ewart GD, Reed KC, Smith GD.** 1990. Soluble hydrogenase of Anabaena cylindrica. Cloning and sequencing of a potential gene encoding the tritium exchange subunit. Eur. J. Biochem. **187**:215–223.
44. **Mahro B, Kusel AC, Grimme LH.** 1986. The significance of hydrogenase activity for the energy-metabolism of green-algae—anaerobiosis favors ATP synthesis in cells of Chlorella with active hydrogenase. Arch. Microbiol. **144**:91–95.
45. **Wu B, Zhang BC, Feng XY, Rubens JR, Huang R, Hicks LM, Pakrasi HB, Tang YJJ.** 2010. Alternative isoleucine synthesis pathway in cyanobacterial species. Microbiology **156**:596–602.
46. **Feng X, Bandyopadhyay A, Berla B, Page L, Wu B, Pakrasi HB, Tang YJ.** 2010. Mixotrophic and photoheterotrophic metabolism in Cyanothece sp. ATCC 51142 under continuous light. Microbiology **156**:2566–2574.
47. **Koropatkin NM, Koppenaal DW, Pakrasi HB, Smith TJ.** 2007. The structure of a cyanobacterial bicarbonate transport protein, CmpA. J. Biol. Chem. **282**:2606–2614.
48. **Douce R, Neuburger M.** 1999. Biochemical dissection of photorespiration. Curr. Opin. Plant Biol. **2**:214–222.
49. **Savage DF, Afonso B, Chen AH, Silver PA.** 2010. Spatially ordered dynamics of the bacterial carbon fixation machinery. Science **327**:1258–1261.
50. **Slack CR, Hatch MD.** 1967. Comparative studies on activity of carboxylases and other enzymes in relation to new pathway of photosynthetic carbon dioxide fixation in tropical grasses. Biochem. J. **103**:660.